chronoabsorptometry will form the substance of a succeeding communication (*15*).

It is apparent from Figure 6 that double potential step methods provide a means for determining both rate constants in the ECEC sequence provided the rate constant ratio lies in the range $0.1 \leq k_2/k_1 \leq 10$. The rate constant $k_1$ can be obtained independently of $k_2$ from an analysis of the forward step charge–time data in a manner analogous to that previously used by Shain (*16*) and by Herman (*17*). Double potential step measurements to define the $|Q_b/Q_f|$ *vs.* $\tau$ behavior will allow determination of the ratio $k_2/k_1$ by a curve-fitting procedure. From a knowledge of $k_1$ and the ratio $k_2/k_1$, the value of $k_2$ can be calculated.

Determination of the temperature dependence of $|Q_b/Q_f|$ at a fixed $\tau$ for the ECEC mechanism is as straightforward as for the EC mechanism only in those special cases where one of the kinetic steps is rate determining, for example, $k_2/k_1 = 0$ and $k_2/k_1 = \infty$. The $|Q_b/Q_f|$ *vs.* temperature profile has already been presented for the $k_2/k_1 = 0$ case in Figure 2. For the cases of intermediate $k_2/k_1$, the best procedure is to calculate $|Q_b/Q_f|$ at each temperature of interest from the finite difference computer program or the results of the analytical equations (*15*).

The extension of these ideas to other electrochemical techniques and reaction mechanisms is straightforward. One must only identify a measurable parameter (see Table III, Reference *1*) whose sole temperature dependence is that of the coupled chemical reaction(s) and apply a graphical analysis analogous to that in Figure 1.

(15) T. H. Ridgway, Ph.D. Thesis, University of North Carolina, Chapel Hill, N.C., 1971.
(16) G. S. Alberts and I. Shain, ANAL. CHEM., **35**, 1859 (1963).
(17) H. B. Herman and H. N. Blount, *J. Phys. Chem.*, **73**, 1406 (1969).

RECEIVED for review March 29, 1971. Accepted August 2, 1971. One of the authors (R.P.V.D.) wishes to acknowledge support of a National Aeronautics and Space Administration Fellowship (1967–70). In addition, various aspects of this work were supported by the Advanced Research Projects Agency under Contract SD-100 with the U.N.C. Materials Research Center and Air Force Office of Scientific Research (AFSC), USAF, Grant AF-AFOSR-69-1625.

# Low-Temperature Electrochemistry

## III. Application to the Study of Radical Ion Decay Mechanisms

**Richard P. Van Duyne[1] and Charles N. Reilley**

*Department of Chemistry, University of North Carolina, Chapel Hill, N.C. 27514*

**The ability of low-temperature techniques to isolate the primary one-electron transfer oxidation or reduction process with a cryoquench of the coupled chemical reactions responsible for the radical ion decay mechanism is demonstrated. Successful cryoquenching, producing radical ion lifetimes of at least 2 sec, was achieved for: a radical anion fragmentation decay reaction (reduction of o- and p-iodonitrobenzene in dimethylformamide); a radical cation dimerization reaction (oxidation of triphenylamine in butyronitrile); a radical cation scavenging reaction by nucleophilic solvent impurity (oxidation of 1,2,3,6,7,8-hexahydropyrene in butyronitrile); and a radical cation scavenging reaction by nucleophilic solvent (oxidation of 9,10-diphenylanthracene in dimethylformamide). In contrast, the lifetime of the 9,10-dimethylanthracene cation radical in butyronitrile is less at low temperatures; the decay reaction involves a prior equilibrium reaction of the cation radical ($DMA^+$) with another cation radical ($DMA^+$) or with parent (DMA) and represents a case where new information has been provided by the low-temperature technique.**

A SURVEY OF THE RECENT literature concerning the preparation and characterization of radical ions indicates that electrochemical methods provide a very facile approach to their generation (*1–4*). The purported reason for this facility of electrochemical radical generation is the ready availability of a controlled potential redox agent (*i.e.*, the electrode) which, in principle, permits a selectivity not easily obtained with chemical redox agents. For example, reduction of an aromatic hydrocarbon with an alkali metal in an ether-type solvent to form the hydrocarbon radical anion is often accompanied by dianion formation due to the large reducing potential of the metal. Electrochemical techniques, however, suffer from the fact that the high dielectric constant, nonaqueous solvents used in electrochemistry, which are capable of supporting a dissociated electrolyte to provide a reasonably low resistance pathway for passage of electrical current, either act as relatively efficient radical ion traps themselves, or they contain notoriously difficult to remove, trace level, impurities that scavenge the radical ions. Recent reviews of oxidative organic electrochemistry (*2, 5*) point out that the chemical fate of an electrogenerated cation radical is frequently dictated by its reaction with residual water in nominally nonaquous solvents. In addition to scavenging by water, radical ions may decay by unimolecular as well as a variety of bimolecular pathways including: unimolecular decomposition (fragmentation) and intramolecular rearrangement, interaction with

[1] Present address, Department of Chemistry, Northwestern University, Evanston, Ill. 60201

(1) "Radical Ions," E. T. Kaiser and L. Kevans, Ed., John Wiley and Sons, New York, N.Y., 1968.
(2) R. N. Adams, "Electrochemistry at Solid Electrodes," Marcel Dekker, New York, N.Y., 1969.
(3) M. E. Peover, "Electrochemistry of Aromatic Hydrocarbons and Related Substances," in "Electroanalytical Chemistry," Vol. 2, A. J. Bard, Ed., Marcel Dekker, New York, N.Y., 1967, pp 1–51.
(4) M. Szwarc, "Carbanions, Living Polymers, and Electron Transfer Processes," Interscience Publishers, John Wiley and Sons, New York, N.Y., 1968.
(5) N. L. Weinberg and H. R. Weinberg, *Chem. Rev.*, **68**, 449 (1968).

**Table I. Cation Radical Decay Reaction Rate Constants and Calculated Activation Energies[a]**

| $R^+$ | Reactant | $k$, $M^{-1}sec^{-1}$ | Decay mechanism | Reference | $E_A$[b] | $E_A$[c] | $E_A$[d] |
|---|---|---|---|---|---|---|---|
| 9,10-DPA[f] | $H_2O$ | $8.3 \times 10^{-2}$ | $^1/_2$ regeneration | *10* | 16.47 | 12.38 | 9.65 |
| 9,10-DPA | $H_2O$ | $6.2 \times 10^{-2}$ | $^1/_2$ regeneration | *11* | 16.64 | 12.56 | 9.83 |
| 9,10-DPA | pyridine | $1 \times 10^4$ | ECE[e] | *12* | 9.55 | 5.45 | 2.73 |
| 9,10-DPA | 4-CN pyridine | $1.3 \times 10^2$ | ECE[e] | *12* | 12.12 | 8.03 | 5.30 |
| 9,10-DPA | 2-Cl pyridine | 5.6 | ECE[e] | *12* | 13.98 | 9.89 | 7.16 |
| TPA[f] | $TPA^+$ | $1.2 \times 10^3$ | ECE | *13* | 10.80 | 6.71 | 3.98 |
| TAA[f] | $CN^-$ | $2 \times 10^5$ | Catalytic | *14* | 7.77 | 3.68 | 0.95 |

[a] Activation energies calculated from Arrhenius equation $k = A \exp(-E_A/RT)$.
[b] $A = 10^{11}\ M^{-1}\ sec^{-1}$.
[c] $A = 10^8 M^{-1}\ sec^{-1}$.
[d] $A = 10^6\ M^{-1}\ sec^{-1}$.
[e] Recent results suggest the strong possibility that this reaction actually proceeds through disproportionation followed by rapid scavenging of dication by the nucleophile (*15*).
[f] 9,10-DPA = 9,10-diphenylanthracene, TPA = triphenylamine, TAA = tri-*p*-anisylamine.

another radical ion or the parent molecule from which the ion was produced, reaction with the solvent, disproportionation (*i.e.*, electron transfer), and reaction with a purposely added reagent. Figure 1 summarizes these decay mechanisms for radical cation reactions where HZ, N:, and $X^-$ are nucleophiles. Although specifically summarizing radical cation reactions, a totally analogous scheme can be formulated for radical anion decay mechanisms by substituting appropriate electrophiles for the nucleophiles.

These decay reactions, while offering fertile ground for study by electroanalytical chemists, are quite deleterious to those interested in preparing stable radicals for optical or ESR spectrometric examination or to those interested in studying the chemiluminescence resulting from anion radical/cation radical annihilation reactions (*6*). In this latter instance, recent work has shown (*7*) that, in certain cases, the products resulting from cation radical scavenging reactions with adventitious water can be excited by energy transfer processes causing them to emit and thereby complicate interpretation of the resulting electrochemiluminescence spectra.

With these ideas in mind, a series of exploratory low-temperature electrochemical studies was initiated using recently developed low-temperature, transient technique methodology (*8*), and diffusion theory (*9*). The principal objective of this work was to demonstrate the ability of low-temperature techniques to isolate the primary one-electron transfer oxidation or reduction process with a cryoquench of the coupled chemical reactions constituting the radical ion decay mechanism. The success of this approach was anticipated in view of the fact that second-order rate constants measured at room temperature for reasonably well established radical cation decay reaction mechanisms were several orders of magnitude below the diffusion controlled limit (*ca.* $10^{10}\ M^{-1}\ sec^{-1}$) for a bimolecular process (Table I).

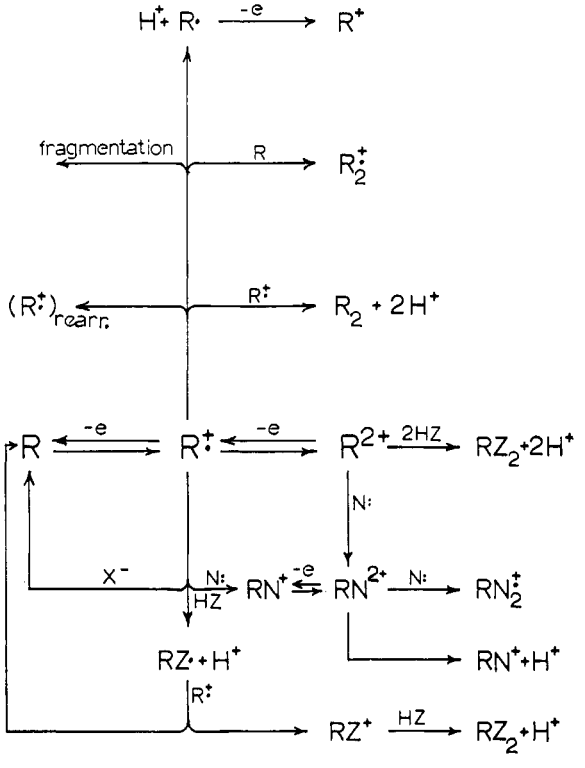


**Figure 1. Mechanisms for radical cation decay reactions**

**R = parent compound; HZ = uncharged nucleophile with acidic proton(s); N: = uncharged nucleophile with lone pair electrons; $X^-$ = nucleophile with full negative charge**

Activation energies calculated from the room temperature rate constants in the table using the Arrhenius equation and the normal value for a bimolecular reaction frequency factor of $10^{11}\ M^{-1}\ sec^{-1}$ (*16*, *17*) are sufficiently large that thermal


(6) D. M. Hercules, *Accounts Chem. Res.*, **2**, 301 (1969).
(7) L. R. Faulkner and A. J. Bard, *J. Amer. Chem. Soc.*, **90**, 6284 (1968).
(8) R. P. Van Duyne and C. N. Reilley, ANAL. CHEM., **43**, 142 (1971).
(9) *Ibid.*, p 153.
(10) R. E. Sioda, *J. Phys. Chem.*, **72**, 2322 (1968).
(11) H. N. Blount and T. Kuwana, *J. Electroanal. Chem.*, **27**, 464 (1970).
(12) G. Manning, V. D. Parker, and R. N. Adams, *J. Amer. Chem. Soc.*, **91**, 4584 (1969).
(13) E. T. Seo, R. F. Nelson, J. M. Fritsch, L. S. Marcoux, D. W. Leedy, and R. N. Adams, *ibid.*, **88**, 3498 (1966).
(14) H. Blount, N. Winograd, and T. Kuwana, *J. Phys. Chem.*, **74**, 3231 (1970).
(15) L. S. Marcoux, *J. Amer. Chem. Soc.*, **93**, 537 (1971).
(16) I. Amdur and G. G. Hammes, "Chemical Kinetics: Principles and Selected Topics," McGraw-Hill Book Co., New York, N.Y., 1966, p 116.
(17) R. A. Marcus, *Can. J. Chem.*, **37**, 155 (1959).

quenching of the decay reactions should be readily effected within the low-temperature range of the butyronitrile and propionitrile solvent systems. If, however, low frequency factors ($10^8$ $M^{-1}$ $sec^{-1}$ or $10^6$ $M^{-1}$ $sec^{-1}$) are encountered for these reactions, as was the case in the series of anion radical protonation reactions studied by Dorfman (*18*), difficulties may be experienced in quenching the faster decay reactions.

In this paper, the low-temperature behavior of several radical ion decay reactions is considered. Each of these is illustrative of one of the radical ion decay pathways in Figure 1 involving interaction between the radical ion and its electrogeneration environment rather than with purposefully added reactants. These studies are continuing, and hopefully more quantitative data concerning the activation parameters of these reactions can be reported in the near future.

## EXPERIMENTAL

**Apparatus.** The apparatus and techniques for the low-temperature cyclic voltammetry and potentiostatic transient experiments have been described elsewhere (*8*).

Bulk coulometry experiments were performed in a three-compartment cell of conventional design having a capacity of 25 ml and an 80 mesh platinum gauze working electrode (*ca.* 10 $cm^2$). The complete electrolysis of 25 ml of 1 m*M* electroactive material required 10–20 minutes with this cell. Magnetic stirring was used in all cases. Current–time data were recorded using a Sargent Model SR strip-chart recorder. The number of Faradays consumed per mole of electroactive species was calculated from the manually integrated current–time curve.

The spectral data for the DPA regeneration experiments were recorded on a Perkin-Elmer 202 UV-VIS spectrophotometer.

The procedures for nonaqueous solvent and supporting electrolyte purification have been described (*8*).

**Reagents.** Nickelocene (Alfa Inorganics) was twice sublimed in vacuo at 70 °C before use.

*Ortho-* and *p*-iodonitrobenzene (Aldrich Chemical Company) were recrystallized twice from 50:50 $EtOH/H_2O$. The ortho isomer was further purified by vacuum sublimation (2×) at 45 °C.

Triphenylamine, 9,10-diphenylanthracene, and 9,10-dimethylanthracene from Aldrich Chemical Company and 1,2,3,6,7,8-hexahydropyrene (Chemical Procurement Laboratories) were used as supplied.

## RESULTS AND DISCUSSION

### RADICAL ANION FRAGMENTATION DECAY REACTIONS

The electrochemical reduction mechanisms of halonitrobenzenes in various nonaqueous solvents have been investigated by Hawley and coworkers (*19*). Consistent with previous ESR studies (*20*), the cyclic voltammetric behavior of the *o*-, *m*-, and *p*-isomers of iodinitrobenzene and *o*-bromonitrobenzene indicated initial formation of the halogenated nitrobenzene anion radical followed by loss of halide ion. Abstraction of an H-atom by the resulting nitrophenyl radical, followed by reduction of nitrobenzene at a slightly more negative potential gave rise to a second voltammetric wave. The mechanism proposed to account for this behavior is:

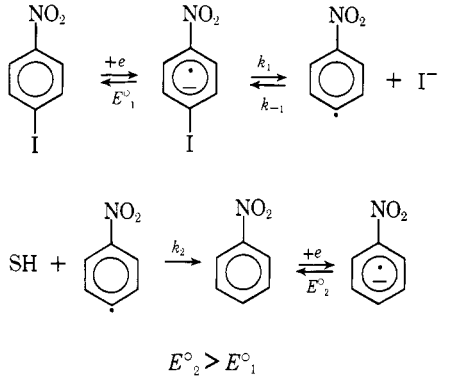


(1)

$$E^\circ_2 > E^\circ_1$$

Addition of halide ion repressed the dissociation of halogenated anion radical except in the case of *o*-bromonitrobenzene. ESR experiments (*21*) employing in situ generation of halogenated nitrobenzene anion radical in deuterated solvent ($CD_3CN$) confirmed H-atom abstraction from solvent rather than from supporting electrolyte cation since *p*-deuteronitrobenzene anion radical was the observed product. Rate constants for the disappearance of halogenated anion radical were measured by reverse current chronopotentiometry treating the system as an EC mechanism (*i.e.*, the transition time occurred at a potential more positive than $E^\circ_2$) and by single potential step chronoamperometry using a potential step amplitude sufficient to encompass both electron transfer processes (*i.e.*, ECE mechanism). The relative rates of the radical anion decomposition are *o*-iodo > *o*-bromo ≫ *p*-iodo > *m*-iodo (500:122:1:0.34). In the chronoamperometry rate measurements, the homogeneous redox reaction:

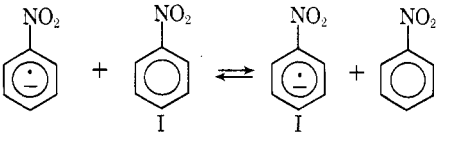


(2)

had to be taken into account in order to extract the rate constant for anion radical decay.

Since these systems studied by Hawley are examples of radical ion fragmentation reactions in general and dissociative electron attachment reactions in particular, which are of considerable importance in radiation chemistry (*22*), negative ion mass spectrometry (*23*), and radical anion cleavage reactions in solution (*24–27*), low-temperature cyclic voltammetry studies of *p*- and *o*-iodonitrobenzene were undertaken in order to see if these thermodynamically unstable species could in fact be stabilized.


(18) S. Arai, E. L. Tremba, J. R. Brandon, and L. M. Dorfman, *Can. J. Chem.*, **45**, 1119 (1967).
(19) J. G. Lawless and M. D. Hawley, *J. Electroanal. Chem.*, **21**, 365 (1969).
(20) T. Kitagawa, T. P. Layloff, and R. N. Adams, ANAL. CHEM., **35**, 1086 (1963).
(21) E. T. Seo and R. F. Nelson, 133rd National Electrochemical Society Meeting, May 1968, Boston, Mass., Abstract No. 207.
(22) W. H. Hamill, "Ionic Processes in γ-Irradiated Organic Solids at −196 °C," in "Radical Ions," E. T. Kaiser and L. Kevan, Ed., John Wiley and Sons, New York, N.Y., 1968, pp 321–416.
(23) R. S. Kiser, "Introduction to Mass Spectrometry and Its Applications," Prentice-Hall, Englewood Cliffs, N.J., 1965.
(24) R. H. Gibson and J. C. Grosthwaite, *J. Amer. Chem. Soc.*, **90**, 7373 (1968).
(25) A. K. Hoffman, W. G. Hodgson, D. L. Maricle, and W. H. Jura, *ibid.*, **86**, 631 (1964).
(26) P. Yousefzadeh and C. K. Mann, *J. Org. Chem.*, **33**, 2717 (1968).
(27) P. Peterson, A. K. Carpenter, and R. F. Nelson, *J. Electroanal. Chem.*, **27**, 1 (1970), and references therein.

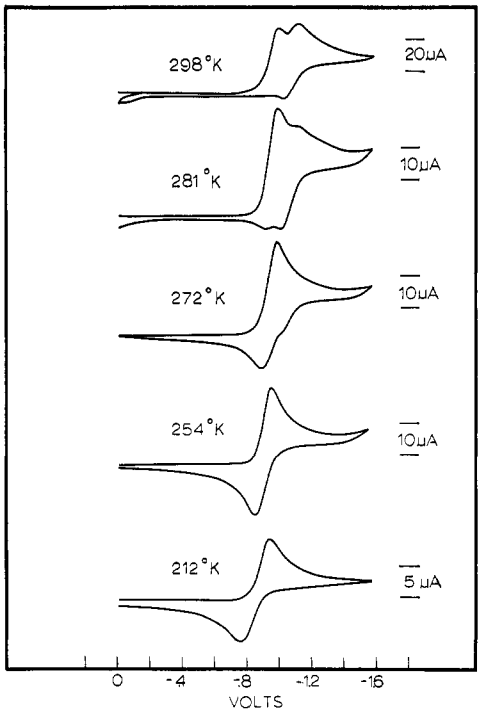


**Figure 2. Low-temperature first sweep cyclic voltammograms of *p*-iodonitrobenzene at a platinum electrode**

**3m*M* *p*-iodonitrobenzene and 0.1*M* TBAP in dimethylformamide at a sweep rate of 135 mV/sec**

Figure 2 shows the cyclic voltammetric behavior of *p*-iodonitrobenzene in dimethylformamide at various subambient temperatures during the cool-down cycle of the electrochemical cryostat. At 298 °K the voltammogram is identical to that previously reported by Hawley (*19*). When cycled between −0.6 V and −1.2 V, sweep rates in excess of 30 V/sec were necessary to completely isolate the $1e^-$ process corresponding to *p*-iodonitrobenzene radical anion formation. Cooling to only 281 °K is sufficient to produce a substantial change in the voltammogram swept at 135 mV/sec. Anodic current due to partial recovery of *p*-iodonitrobenzene anion radical is clearly seen. Qualitatively the relative anodic and cathodic peak currents of the 281 °K voltammogram are similar to those in Hawley's room temperature experiment in which 0.1*M* tetraethylammonium iodide (TEAI) was substituted for TEAP indicating a comparable suppression of the radical anion decomposition. Further cooling results in increased recovery of *p*-iodonitrobenzene radical anion during the reverse sweep until at 254 °K the criteria for chemical reversibility by cyclic voltammetry ($i_p^a/i_p^c = 1.0$ and $i_p^c V^{c-1/2}/C$ = constant) are fulfilled. Double potential step chronoamperometry and chronocoulometry experiments at 254 °K where the potential was stepped from −0.7 V to −1.2 V *vs.* SCE confirm the chemical stability of the *p*-iodonitrobenzene radical anion for at least 2.0 sec. The anodic–cathode peak potential separation at this temperature under optimal *iR* compensation conditions was, however, slightly greater than the theoretically predicted value of *ca.* 52 mV from Figure 4 of Reference *9* (80 mV measured). Lowering the temperature to 212 °K resulted in a further increase in radical anion lifetime and anodic–cathodic peak potential separation. At 212 °K the sweep rate could be lowered to 10 mV/sec without causing $i_p^a/i_p^c$ to deviate from 1.0 indicating the radical anion lifetime had increased to *ca.* 30 sec. The anodic–cathodic peak potential separation at 212 °K may be due to thermal

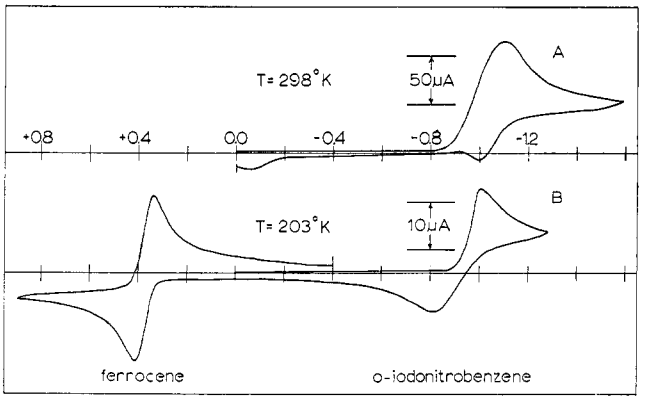


**Figure 3. First-sweep cyclic voltammograms of *o*-iodonitrobenzene and ferrocene at a platinum electrode**

**3.24mM *o*-iodinitrobenzene, 3.22m*M* ferrocene, and 0.1*M* TBAP in dimethylformamide at a sweep rate of 200 mV/sec**
***A*. 398 °K**
***B*. 203 °K**

attenuation of the heterogeneous rate constant. Double potential step chronocoulometry experiments at 212 °K indicate that adsorption of electroactive species is less than $5 \times 10^{-12}$ mole/cm$^2$. The anodic–cathodic peak potential separation is a function of sweep rate in the manner expected for a slow charge transfer process and it is not a function of *p*-iodonitrobenzene concentration over the range 1–4 m*M* which indicates that the separation is not solely an *iR* drop manifestation. We are not able at this time to rule out the possibility of nonelectroactive species adsorption which acts as an electron transfer blocking agent.

Iodide loss from *o*-iodonitrobenzene is 500 times faster than for the para isomer (*19*). The room temperature cyclic voltammetric behavior of *o*-iodonitrobenzene is shown in Figure 3*A*. The broadness of the main reduction wave results from a lack of resolution of the *o*-iodonitrobenzene and nitrobenzene reduction processes. At sweep rates up to 100 V/sec, no recovery of *o*-iodonitrobenzene radical anion could be observed; however, by cooling to 233 °K, partial recovery was obtained at sweep rates as low as 200 mV/sec. At 203 °K, Figure 3*B*, virtually complete recovery of *o*-iodonitrobenzene radical anion was extant as indicated by the equal number of coulombs passed under the forward sweep and reverse sweep waves. This integration was carried out manually. Double potential step chronocoulometry measurements confirmed this result. $|Q_b/Q_f| = 0.569$ (0.586 theoretical) was obtained when the potential was stepped between −0.6 V and −1.2 V for $\tau$ from 1.0 sec to 0.020 sec. The anodic–cathodic peak potential separation of *o*-iodonitrobenzene at 203 °K was *ca.* 200 mV and is indicative of a slow charge transfer process. This is readily apparent in Figure 3*B* where ferrocene has beeen added as an *iR* drop internal standard. The anodic–cathodic peak potential separation of the ferrocene is much closer to the theoretical value than is that for *o*-iodonitrobenzene.

Future low-temperature studies of these dissociative anion radical decay reactions will be concerned with the measurement of their activation parameters using the theory and techniques previously outlined (*8*, *9*). An important consideration in carrying out these measurements will be the extent to which the temperature dependence of the homogeneous electron exchange reaction 2 perturbs the temperature dependence of the ECE reaction sequence 1. If it is an important factor, a family of ECE working curves will have to be digitally simulated to represent the temperature dependence of the equilibrium constant for Reaction 2. Following the determination

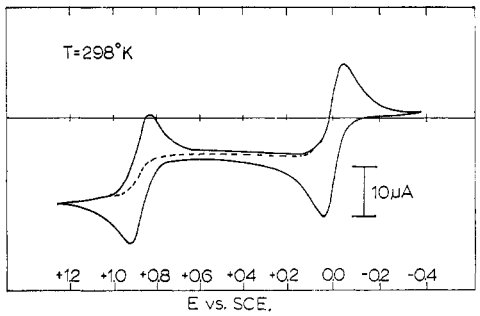


**Figure 4. Steady-state cyclic voltammograms of nickelocene at a platinum electrode**

**——, 2.0m*M* nickelocene and 0.1*M* TEAP in "dry" (≤3m*M* $H_2O$) acetonitrile; - - - - - -, 2.0m*M* nickelocene and 0.1*M* TEAP in wet (*ca.* 50 m*M* of $H_2O$) acetonitrile. Sweep rate = 100 mV/sec. *T* = 298 °K**

of reliable activation parameters over a wide temperature range, it should be possible to interpret the measured activation entropy to ascertain whether H-atom abstraction (an associative process, $\Delta S^{\ddagger} = -$) or radical anion dissociation ($\Delta S^{\ddagger} = +$) is the rate determining step in the decay reaction.

## RADICAL CATION SCAVENGING BY NUCLEOPHILIC SOLVENT IMPURITIES

**Oxidation of Nickelocene in Acetonitrile.** Hawthorne *et al.* (*28*) were able to oxidize nickelocene to a formally $d^6$ Ni(IV) dication species, $(\pi\text{-}C_6H_5)_2Ni^{2+}$, using low-temperature cyclic voltammetry. Other $d^6$ bis(cyclopentadienyl) metallocenes, ferrocene and cobalticinium ion, are exceptionally stable species, ostensibly because they are electronically stabilized because of retention of an inert gas electronic configuration around the central metal atom. Earlier attempts to form the Ni(IV) dication by electrolytic oxidation in ethanolic media were frustrated by complete decomposition of the oxidized products (*29*). The question naturally arises then as to the nature of the follow-up chemical reaction which prevents observation of a stable Ni(IV) species. Does $(\pi\text{-}C_6H_5)_2Ni^{2+}$ unimoleculary decompose (*i.e.*, is it inherently unstable thermodynamically) in which case it will serve admirably as a low-temperature system for studying dissociative electron withdrawal reactions or does it merely react rapidly with some trace constituent of its electrogeneration environment? In analogy with the electrochemical oxidation of aromatic hydrocarbons, where residual water is a sufficiently strong nucleophile in nonaqueous solvents to rapidly scavenge radical cations and dications, water was suspected as being the scavenging agent for the Ni(IV) species.

This hypothesis was tested by measuring the room temperature cyclic voltammogram of nickelocene in the driest acetonitrile available (<2m*M* $H_2O$). The nickelocene/TEAP solution was prepared by vacuum line techniques to avoid oxygen and water contamination. The acetonitrile was thoroughly degassed by repetitive freeze–pump–thaw cycles, since nickelocene is extremely sensitive to decomposition in the presence of molecular oxygen. After preparation, the nickelocene test solution was brought to atmospheric pressure under highest purity nitrogen and transferred by nitrogen pressure to a thoroughly dried electrochemical cell. Figure 4 compares the

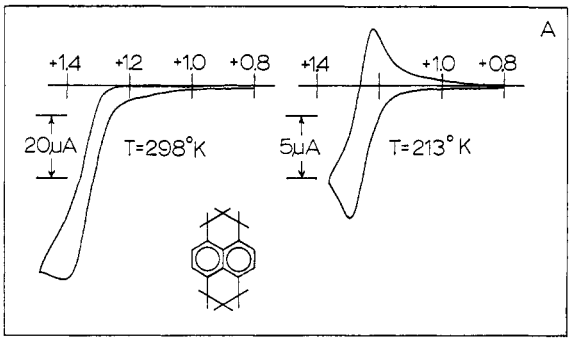


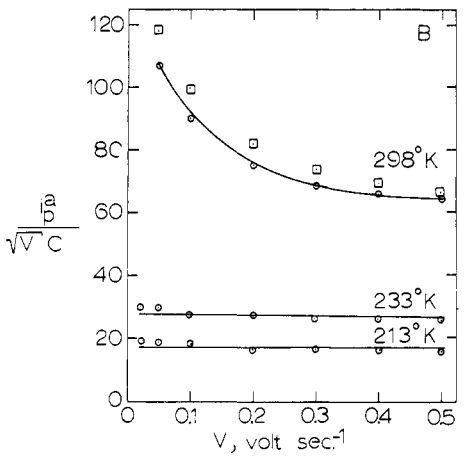


**Figure 5. Cyclic voltammetric vehavior of 1,2,3,6,7,8-hexahydropyrene in butyronitrile at a platinum electrode**

***A*. 2.52m*M* hexahydropyrene and 0.1*M* TBAP in butyronitrile at *T* = 298 °K and *T* = 213 °K. Sweep rate = 50 mV/sec**

***B*. Cyclic voltammetric sweep rate study as a function of temperature**

**⊙ 2.52m*M* hexahydropyrene**

**⊡ 3.58m*M* hexahydropyrene**

cyclic voltammetric behavior of nickelocene under "dry" and wet (*ca.* 50m*M* $H_2O$) conditions. With the vacuum line prepared sample, two highly reversible, both chemically and electrochemically, oxidation waves were observed. Both waves conformed well to the usual cyclic voltammetric criteria for a reversible process. The nickel(IV) dication was, in fact, sufficiently stable that $i_p^c/i_p^a = 1.0$ pertained for sweep rates as low as 0.010 *V*/sec. Double potential step chronocoulometry and chronoamperometry confirmed the stability of the Ni(IV) dication under these "dry" conditions.

These results show that the Ni(IV) dication is a highly reactive species rather than a thermodynamically unstable one. The rapid nucleophilic reaction with water suggests that this is also the reason that previous workers failed to observe Ni(IV) dication in ethanol since ethanol is also a good nucleophile. Low-temperature electrochemistry, although not absolutely necessary to demonstrate the existence of Ni(IV) dication, since water could have been reduced to a sufficiently low level, will be useful in attempts to isolate it. For example, low-temperature electrolysis in rigorously purified liquid sulfur dioxide/0.1*M* TBAP (*30*) to generate the $Ni(IV)^{2+}$ followed by evaporation of $SO_2$ still at low-temperatures should allow the $Ni(IV)^{2+}$/TBAP residue to be redissolved in an easily dried solvent such as 1,2-dimethoxyethane and, thus, be isolated for spectrometric or magnetic examination.

(28) R. J. Wilson, L. F. Warren, and M. F. Hawthorne, *J. Amer. Chem. Soc.*, **91**, 758 (1969).

(29) G. Wilkinson, P. L. Pauson, and F. A. Cotton, *ibid.*, **76**, 1970 (1954).

(30) L. L. Miller and E. A. Mayeda, *ibid.*, **92**, 5818 (1970).

**Oxidation of 1,2,3,6,7,8-Hexahydropyrene in Butyronitrile.** The oxidation of 1,2,3,6,7,8-hexahydropyrene (HHP) has been investigated previously by Marcoux (*31*) who demonstrated that a relatively stable (*ca.* 1–5 sec) HHP cation radical could be electrogenerated in nitrobenzene solvent. HHP can be considered as a 1,4,5,8-tetraalkylated naphthalene and since the reactive $\alpha$ positions of the "naphthalene" moiety are blocked, a stable cation radical is not unexpected. In acetonitrile (<3m*M* $H_2O$), however, we have observed greatly reduced stability by cyclic voltammetry ($i_p^c/i_p^a$ = 1.; only for sweep rates > *ca.* 20 V/sec). Sweep rate studies indicate an ECE-type decay reaction, probably involving residual water as usual. In butyronitrile (Figure 5*A*) at room temperature, sweep rates in excess of 5 V/sec were necessary to achieve $i_p^c/i_p^a$ = 1.0 for 2.52m*M* HHP. The value of $i_p^c/i_p^a$ at a given sweep rate was a function of HHP concentration. Somewhat greater cation radical stability was found at higher (3–5-m*M*) HHP concentrations indicating that the scavenging agent concentration is probably in the 0.5 to 2m*M* range (residual water again?). The room temperature $i_p^a V^{-1/2}/C$ *vs.* V behavior is indicated in Figure 5*B* and is typical of an ECE decay reaction. No HHP regeneration has been detected either electrochemically or spectrophotometrically.

Cooling to 213 °K results in a completely stable HHP cation radical for sweep rates as low as 0.02 V/sec. Cryoquenching of the follow-up decay reaction is manifested in the sweep rate study (Figure 5*B*) by the constant value of $i_p^a V^{-1/2}/C$ as a function of sweep rate. Double potential step chronocoulometry at 213 °K confirms that the decay reaction has been completely quenched for at least 2.0 sec since $|Q_b/Q_f| = 0.57$ was obtained for 0.050 sec $\leq \tau \leq$ 1.0 sec. This is the most highly temperature dependent cation radical decay reaction we have encountered to date.

## RADICAL CATION SCAVENGING BY NUCLEOPHILIC SOLVENT

The oxidative and reductive electrochemistry of 9,10-diphenylanthracene (DPA) have been extensively examined in recent years primarily due to interest in the intense annihilation electrochemiluminescence (ECL) observed when a $DPA^-$ and a $DPA^+$ are diffusionally mixed (*6*). Thorough understanding of the nature of this luminescence is contingent upon understanding the chemical interactions of $DPA^+$ and $DPA^-$ with their respective electrogeneration environments. The DPA radical anion has been shown to be stabile for 60–80 minutes (in dimethylformamide) when generated in the strict absence of proton donor species (*32*). In contrast, the cation radical is considerably less stable. Sioda (*10*) has discussed the chemical and spectrometric properties of $DPA^+$ demonstrating that its instability in acetonitrile is due to a relatively slow nucleophilic reaction with residual water. The product of this hydrolysis is *trans*-9,10-dihydro-DPA-9,10-diol formed with overall $^1/_2$ regeneration stoichiometry:

$$2\ DPA^+ + 2\ H_2O \rightarrow DPA + DPA(OH)_2 + 2\ H^+ \quad (3)$$

This mechanism has been fairly well established by several subsequent investigations (*11*, *33*, *34*). The rate data obtained for the hydrolysis of $DPA^+$ are listed in Table I. $DPA^+$ has also been electrogenerated and studied by cyclic voltammetry in methylene chloride (*35*), nitrobenzene (*36*), liquid sulfur dioxide (*30*), butyronitrile (*37*), and dimethylformamide (*38*). Cation radical lifetimes in excess of 5 sec have been observed in all these solvents with the exception of dimethylformamide.

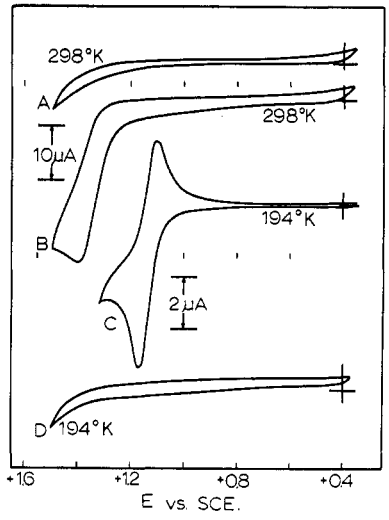


**Figure 6. First-sweep cyclic voltammograms at a platinum electrode**

*A.* **0.1*M* TBAP in dimethylformamide background**
*B.* **Same as *A* with 3.35m*M* 9,10-diphenylanthracene added**
*C.* **Same as *B* but *T* = 194°K**
*D.* **Same as *A* but *T* = 194 °K**
**Sweep rate = 135 mV/sec**

Previous investigations have reported the instability of $DPA^+$ in dimethylformamide. Sioda (*10*) noted that $DPA^+$ apparently reacted with dimethylformamide in an analogous manner to its reaction with water since partial regeneration of DPA was observed. Cruser and Bard (*38*) studied the lifetimes of several radical cations in dimethylformamide using the intensity–time dependence of the annihilation ECL emission as a kinetic probe. The radical cations generated from DPA, rubrene, and tetraphenylpyrene were investigated. In order to quantitatively relate the observed intensity–time profile to the cation radical lifetime, a pseudo first order following chemical reaction giving nonelectroactive products was assumed as the decay reaction and a Feldberg-type digital simulation approach was applied. Using this technique, two different $DPA^+$ decay rate constants were measured, 225 $sec^{-1}$ and 140 $sec^{-1}$, depending on the method of data analysis chosen.

Since dimethylformamide is frequently used for electrochemiluminescence studies (*7*, *39*) presumably because it can be highly purified, high molecular weight hydrocarbons are quite soluble in it, and aromatic hydrocarbon radical anions are very stable in DMF; and because the $DPA^+$/DMF interaction is a clear example of an electrogenerated species being scavenged by the solvent, low-temperature electrochemical studies were initiated to investigate the thermal quenching possibilities for this decay reaction. Figure 6 illustrates the

(31) L. S. Marcoux, Ph.D. Thesis, University of Kansas, Lawrence, Kan., 1967.
(32) K. S. V. Santhanam and A. J. Bard, *J. Amer. Chem. Soc.*, **88**, 2669 (1966).
(33) P. T. Kissinger and C. N. Reilley, ANAL. CHEM., **42**, 12 (1970).
(34) G. C. Grant and T. Kuwana, *J. Electroanal. Chem.*, **24**, 11 (1970).
(35) J. Phelps, K. S. V. Santhanam, and A. J. Bard, *J. Amer. Chem. Soc.*, **89**, 1752 (1967).
(36) L. S. Marcoux, J. M. Fritsch, and R. N. Adams, *ibid.*, p 5766.
(37) R. P. Van Duyne, University of North Carolina, Chapel Hill, N.C., unpublished results, 1969.
(38) S. A. Cruser and A. J. Bard, *J. Amer. Chem. Soc.*, **91**, 267 (1969).
(39) C. A. Parker and G. D. Short, *Trans. Faraday Soc.*, **36**, 2618 (1967).

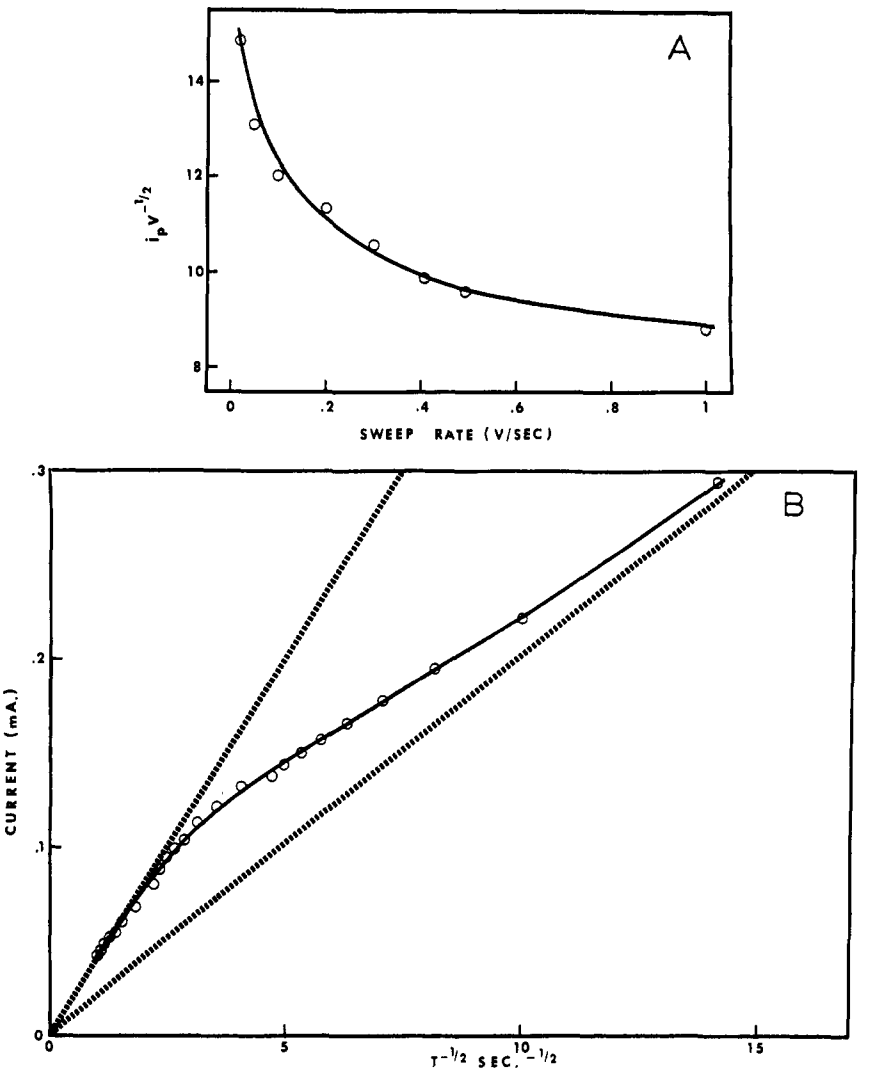


**Figure 7. Cyclic voltammetry sweep rate studies (*A*) and single potential step chronoamperometry (*B*) of the oxidation of 2.94m*M* 9,10-diphenylanthracene and 01.*M* TBAP in dimethylformamide at a platinum electrode**

*A*. First sweep data, $T$ = 298 °K
*B*. Dotted lines are 1*e* and 2*e* transfer limiting cases, potential step amplitude +1.00 V to +1.44 V *vs.* SCE, $T$ = 298 °K

first sweep cyclic voltammetric behavior for the oxidation of DPA to its monocation radical in dimethylformamide. At room temperature, oxidation of DPA occurs at +1.35 V *vs.* SCE with no recovery of DPA cation radical on the reverse potential sweep at 0.135 V/sec. Increasing the sweep rate to *ca.* 50 V/sec resulted in complete $DPA^+$ recovery (*i.e.*, $i_p^c/i_p^a$ = 1.0). Cooling to 194 °K, which is well into the dimethylformamide supercooling region, also results in complete stabilization of the cation radical ($i_p^c/i_p^a$ = 1.00 and $i_p^a$ $V^{-1/2}/C$ = constant) for sweep rates in excess of 0.025 V/sec. Background voltammograms are included in Figure 6 for comparison. Since rubrene and tetraphenylpyrene radical cations are less reactive than DPA radical cation, low-temperature quenching should also be effective in eliminating their undesirable decay reactions. Further investigations of these systems under low-temperature conditions are in progress to determine more quantitatively the thermal response of these cation radical–dimethylformamide decay reactions.

The apparent discrepancy between the regenerative mechanism proposed by Sioda (*10*) for the $DPA^+$/dimethylformamide decay reaction and the EC mechanism assumed by Bard (*38*) for measurement of the $DPA^+$ lifetime stimulated a more complete investigation of this decay mechanism. Additionally it is noted that the discrepancies between the pseudo first order decay rate constants measured by various methods of ECL data analysis coupled with the fact that the one-electron oxidation of $DPA^+$ should not be isolated by a sweep rate of only 50 V/sec if the follow-up reaction has a rate constant on the order of 225 $sec^{-1}$ or 140 $sec^{-1}$ cast doubt on Bard's EC mechanism. Figure 7*A* shows the results of a cyclic voltammetric sweep rate study. The substantial decrease in the peak current function with increasing sweep rate is consistent with either an ECE, catalytic, or fractional regeneration decay mechanism (*40*). Single potential step chronoamperometry experiments, in which the potential is stepped from +1.00 V where no oxidation takes place to +1.44 V where DPA oxidation takes place at a diffusion controlled rate, indicate a transition between an overall 2 $e^-$ oxidation at long times and a 1 $e^-$ oxidation at short times. This type of "break-over" behavior in the current *vs.* $t^{-1/2}$ plot is indicative of an ECE reaction sequence (*41*) or a $^1/_2$ regeneration sequence (*42*). It is clearly not consistent with a catalytic mechanism (*43*) since a steady state current at long times which is independent of time was not observed over an interval of 2.0 sec at which time spherical diffusion and convection problems interfere with the application of planar diffusion theory. Confirmation of the 2 $e^-$ oxidation process at long times was obtained from controlled potential coulometry experiments in neat DMF.

(40) R. Nicholson and I. Shain, ANAL. CHEM., **36**, 706 (1964).
(41) G. S. Alberts and I. Shain, *ibid.*, **35**, 1859 (1963).
(42) R. Guidelli and D. Cozzi, *J. Electroanal. Chem.*, **14**, 245 (1967).
(43) P. Delahay and G. L. Stiehl, *J. Amer. Chem. Soc.*, **74**, 3500 (1952).

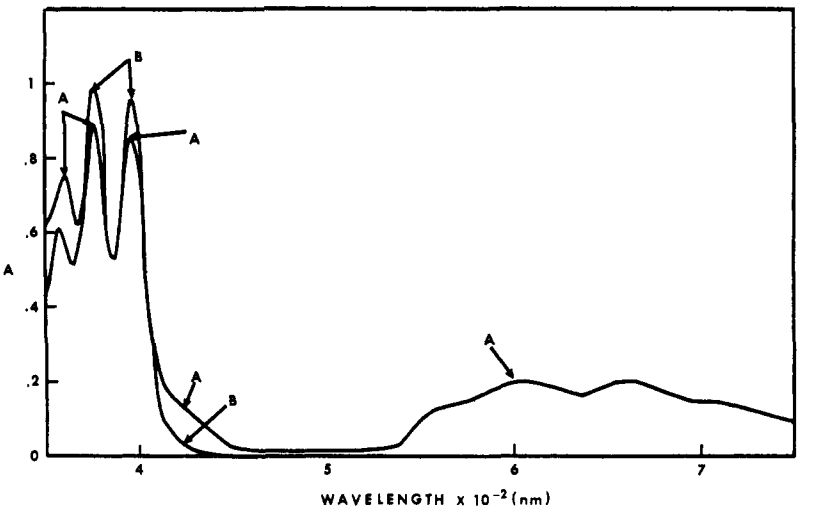


**Figure 8. Visible spectra of 1.0m*M* 9,10-diphenylanthracene and 0.1*M* TBAP in methylene chloride**

*A*. After electrolysis at +1.3 V *vs.* SCE for 2.0 min
*B*. after addition of excess (200 μl) dimethyformamide

It should be noted, however, that in mixed DMF/acetonitrile media where the $DPA^{+}$/DMF decay reaction is much slower than in neat DMF solvent, more than 2 Faradays/mole of DPA were consumed, indicating that there may be slower secondary reactions involving electroactive products in the overall decay reaction scheme.

Although a quantitative difference does exist between the working curves for the ECE and $^1/_2$ regeneration mechanisms, rather precise chronoamperometric data are required to distinguish the two mechanisms. Since a computer data acquisition facility, required to obtain measurements of this precision, was not available at the time, a simple spectrophotometric experiment served to detect any possible regeneration of DPA. $DPA^{+}$ was electrogenerated for *ca.* 2 minutes in spectroquality methylene chloride, where the water scavenging process, Reaction 3, is quite slow due to the low water content of $CH_2Cl_2$. Curve *A* in Figure 8 is the visible spectrum of this partially electrolyzed solution. Unoxidized DPA absorbs at 376 nm and 396 nm essentially free from $DPA^{+}$ absorption while $DPA^{+}$ absorbs exclusively between 420–430 nm and 550–750 nm. Addition of excess dimethylformamide (200 μl) to this DPA/$DPA^{+}$ solution, Curve *B*, Figure 8, resulted in "instantaneous" decay of the cation radical absorption bands and a concomittant increase in the DPA bands at 376 and 396 nm. In a separate experiment spanning the same elapsed time as the dimethylformamide addition experiment, it was determined that less than 5% of the observed DPA regeneration could be attributed to the water decay reaction.

The possibility exists that the decay reaction actually measured involves reaction of $DPA^{+}$ with trace water or one of the decomposition products of dimethylformamide (*e.g.*, dimethylamine). Evidence against this hypothesis is that no impurities could be detected by gas chromatography in the dimethylformamide used with either a thermal conductivity detector or a flame ionization detector, and that the water decay reaction is so slow (*10*) that the amount of water escaping GC detection (*ca.* 1m*M*) could at most account for the loss of a very small fraction of the electrogenerated $DPA^{+}$; and that there was no DPA concentration dependence of the cation radical lifetime as measured by cyclic voltammetry and chronoamperometry indicating that the $DPA^{+}$ scavenging agent concentration is much greater than the local $DPA^{+}$ concentration.

It is thus asserted that the decay reaction of $DPA^{+}$ with dimethylformamide is of the $^1/_2$ regeneration type. Fitting the chronoamperometric data of the $^1/_2$ regeneration working curve calculated from Equation 22 of Reference *38* results in a

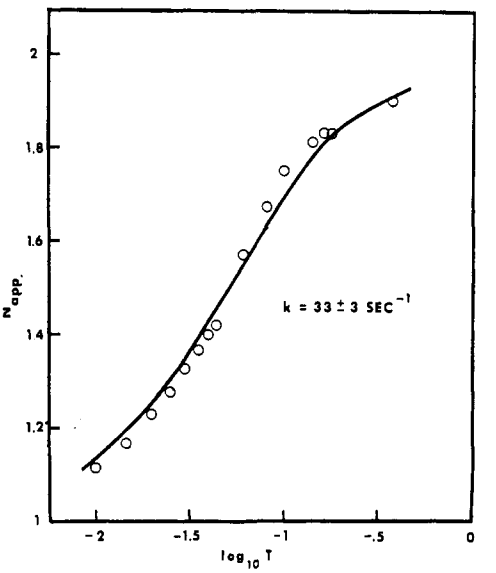


**Figure 9. Comparison of experimental single potential step chronoamperometry data for the oxidation of 2.94m*M* 9,10-diphenylanthracene and 0.1*M* TBAP in dimethylformamide with the theoretical working curve for the pseudo-first order $^1/_2$ regeneration mechanism**

**Potential step amplitude +100 V to +1.44 V *vs.* SCE**

pseudo first order rate constant of 33 ± 3 $sec^{-1}$ or a second-order rate constant of 2.27$M^{-1}$ $sec^{-1}$ based on a neat dimethylformamide concentration of 14.5*M* (Figure 9). This value for the pseudo first order rate constant is a factor of 4 smaller than that reported by Bard (*38*) and is consistent with the cyclic voltammetric results.

In analogy with the mechanism proposed by Sioda (*10*) for the hydrolysis of $DPA^{+}$, we offer the following scheme for the $DPA^{+}$/DMF decay reaction:

$$DPA \rightleftharpoons DPA^{+} + e^{-} \qquad (4)$$

$$DPA^{+} + (Me)_2NCH(=O) \xrightarrow{k_1} \text{(I)} + CO \qquad (5)$$

(I) = $C_6H_5$, $NH(Me)_2$ $ClO_4^{-}$, $C_6H_5$

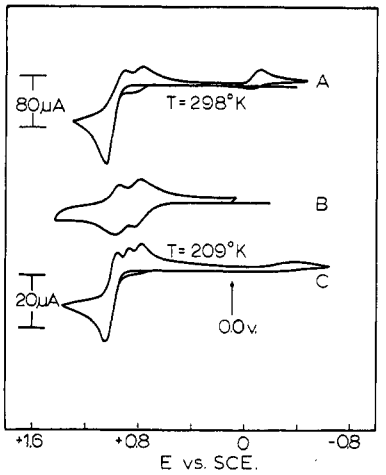


**Figure 10. First sweep cyclic voltammograms of triphenylamine at a platinum electrode**

*A.* **4m*M* triphenylamine and 0.1*M* TBAP in butyronitrile. Sweep rate = 100 mV/sec**
*B. ca.* **0.5m*M* tetraphenylbenzidine and 0.1*M* TEAP in acetonitrile from Adams, *J. Amer. Chem. Soc.*, 88, 3498 (1966)**
*C.* **Same as *A* but at low temperature. Note potential axis displacement**

$$I + DPA^{+\cdot} \xrightarrow{k_2} \text{(II)} + DPA \quad (6)$$

where: $k_2 >> k_1$; $k_{obsd} = 2k_1$

$$II + DMF \xrightarrow{k_3} \text{(III)} + CO \quad (7)$$

Although we have no positive product identification at this time to verify (or dispute) this proposed mechanism, the following evidence is available in addition to the above verification of the $^1/_2$ regeneration nature of the decay scheme: no free $H^+$ wave is observed near 0.0 volts in the cyclic voltammetry of DPA in DMF; voltammetry of solutions resulting from the controlled potential electrolysis of DPA in neat DMF at +1.45 V *vs.* SCE show one main product wave near −0.5 V *vs.* SCE [The shape and potential of this wave are virtually identical to that reported by Manning for reduction of the salt 9,10-diphenylanthracene-9,10-dipyridinium perchlorate (*44*)]; and the decarbonylation of DMF following its attack on the positively (partial) charged carbon atom of various halobenzimidazoles has been reported (*45*). Both the first and second assertions are consistent with the proposal that 9,10-diphenylanthracene-9,10-bis(dimethylammonium)perchlorate(III) is the overall oxidation product. Perhaps one of the most useful means of verifying the $DPA^{+\cdot}$/DMF reaction mechanism will be the following: generate $DPA^{+\cdot}$ using low-temperature electrolysis in liquid $SO_2$ as per Reference *24;* isolate the radical cation salt by $SO_2$ evaporation; and after DMF addition follow the decay kinetics of $DPA^{+\cdot}$ homogeneously (spectrophotometrically) in the manner advocated by Shine (*46*).

(44) G. Manning, Ph.D. Thesis, University of Kansas, Lawrence, Kan., 1969.
(45) L. Joseph and A. H. Albert, *J. Heterocycl. Chem.*, **3**, 107 (1966).

## RADICAL CATION DIMERIZATION AND/OR RADICAL CATION-PARENT DECAY REACTION

**Oxidation of Triphenylamine in Butyronitrile.** The oxidative electrochemistry of triphenylamine (TPA) and a wide variety of substituted triphenylamines in acetonitrile has been examined in detail by Adams and associates (*13*, *47*). For the fully tri-para-substituted compounds, reversible one-electron oxidations occur generating stable monocation radicals with no apparent follow-up chemical reactions. On the other hand, rapid coupling reactions occur with unsubstituted or partially parasubstituted triphenylamines forming the corresponding tetraphenylbenzidines (TPB) which in turn can be electrooxidized to diquinoid species at potentials more positive of that required to oxidize the starting TPA. Characterization of the follow-up reaction sequence by macroscale electrolysis (coulometry) and subsequent product identification, by optical and ESR spectrometry, and by cyclic voltammetry and chronopotentiometry has resulted in the following oxidation mechanism as written for TPA:

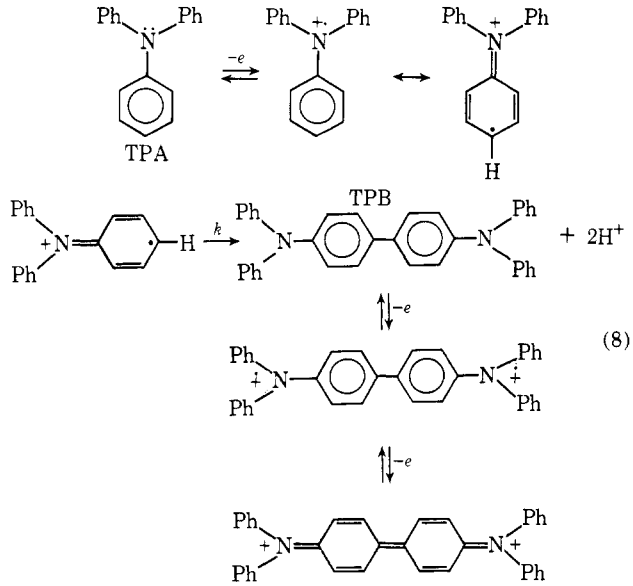


Recently, the cation radical dimerization rate constants for this second-order ECE mechanism have been measured by chronoamperometry (*48*) $k = 1.2 \times 10^3 \pm 0.33M^{-1}$ sec$^{-1}$ (TPA), and by rotating disk voltammetry (*49*) $k = 3 \times 10^3 \pm 0.9M^{-1}$ sec$^{-1}$ (TPA). As a result of the large amount of work done on triphenylamine and substituted TPA systems, it emerges as one of the best characterized nonaqueous electrochemical mechanisms.

In view of the wide spread occurrence of cation radical coupling involving aromatic amines (*50*), the low-temperature electrochemistry of triphenylamine was investigated in order to determine if the activation energy for the dimerization reaction was sufficient to permit thermal blocking of the normal cation radical decay pathway. The first sweep cyclic voltammetric behavior of triphenylamine in butyronitrile is given in Figure

(46) Y. Murata and H. J. Shine, *J. Amer. Chem Soc.*, **91**, 1872 (1969).
(47) R. F. Nelson and R. N. Adams, *ibid.*, **90**, 3925 (1968).
(48) R. F. Nelson and S. W. Feldberg, *J. Phys. Chem.*, **73**, 2623 (1969).
(49) L. S. Marcoux, R. N. Adams, and S. W. Feldberg, *ibid.*, p 2611.
(50) R. N. Adams, *Accounts Chem. Res.*, **2**, 175 (1969).

10. The overall morphology of the voltammetric waves observed at room temperature, *A*, is identical to that previously reported for TPA in acetonitrile (*13*) although all the peak potentials are shifted *ca.* 70 mV more positive in butyronitrile (SCE reference electrode in both solvents). This probably reflects a liquid junction potential difference between the two solvents. The two oxidation–reduction peaks of tetraphenylbenzidine, *B*, appear only after the first sweep causing oxidation of TPA. The wave near 0.0 V is the reduction of free protons liberated in the $TPA^+$ coupling reaction. The dimerization rate constant for TPA in butyronitrile has not yet been measured quantitatively; however, qualitative indications are that changing solvents from acetonitrile to butyronitrile does not drastically alter this rate. By assuming the dimerization rate constant measured in acetonitrile ($3 \times 10^3 M^{-1}$ $sec^{-1}$) pertains, the TPA cation radical lifetime under the concentration conditions of Figure 10 is *ca.* 80 msec.

Cooling the butyronitrile solvent to 209 °K while maintaining the sweep rate at 100 mV/sec, one observes a growing in of a reverse sweep cathodic current, *C*, corresponding to reductive recovery of TPA monocation radical. Thus at 209 °K three reduction waves are observed during the reverse potential sweep. Increasing the sweep rate to 10 V/sec at the low-temperature resulted in a single one-electron reversible wave for the oxidation of TPA and the complete recovery of TPA cation radical. Double potential step chronocoulometry experiments were carried out (Figure 11) with the potential step amplitude set to encompass both the $TPA/TPA^+$ and $TPB/TPB^{2+}$ couples. This coupled chemical reaction system is the second order kinetic analog of the ECEC mechanism with $k_2/k_1 = 0$ case discussed in Reference *9*. Since $TPB^{2+}$ is a very stable species in acetonitrile (*13*) and presumably is also stable in butyronitrile, an overall two-electron transfer should occur during the anodic potential step, provided $\tau$ is large compared with the radical cation lifetime, and one electron/TPA should be recovered because of the reduction of $TPB^{2+}$ on the reverse potential step. This behavior is manifested in a double potential step chronocoulometry experiment by the $|Q_b/Q_f|$ ratio approaching approximately $1/2$ of its reversible one-electron value at long $\tau$. The chronocoulometric data taken at room temperature in Figure 11 are clearly consistent with this type of behavior. Cooling to 183 °K is effective in stabilizing the monocation radical (*i.e.*, quenching the normal decay reaction) for periods of at least 2.0 sec (corresponding to 2 $\tau$) as indicated by a $|Q_b/Q_f|$ value of 0.60 at $\tau C_A^* = 242 \times 10^{-5} M$ sec. This represents at least a sixfold increase in the radical cation lifetime.

Having effected a thermal quench of the normal cation radical decay pathway, the possibility exists for studying the decay reaction of the free cation radical with purposefully added nucleophiles at low temperatures. The electrical excitation signal frequency can then be varied to change the reaction time gate.

**Oxidation of 9,10-Dimethylanthracene in Butyronitrile.** A survey of the DMA electrochemical literature reveals that:

$DMA^-$ is very stable in acetonitrile and DMF

$DMA^+$ is much less stable than the anion. $DMA^+$ is more stable in nitrobenzene (*36*) than in acetonitrile (*51–53*) but is very unstable in DMF on the cyclic voltammetry time scale (*39*). For more prolonged periods $DMA^+$ probably decays by a $H_2O$ scavenging process.

In the presence of a relatively strong nucleophile (*e.g.*, acetate), a dimeric DMA acetate IV

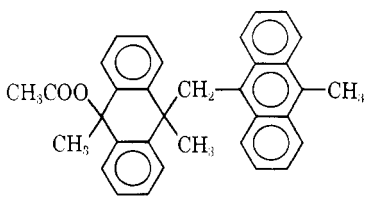


IV

can be isolated from a controlled potential electrolysis in $CH_4CN$ at +1.1 V *vs.* SCE (*53*).

From the oxidation of DMA in the presence of 2,6-lutidine, which acts as a base rather than as a nucleophile, the dimer V

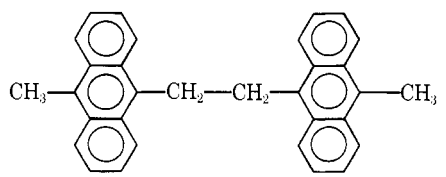


V

can be isolated (*54*).

The room temperature cyclic voltammetric behavior of DMA in butyronitrile over the potential range +1.3 V to −2.3 V is illustrated in Figure 12*A*. Scanning anodically, one first observes the oxidation peak, 1, at +1.17 V (compared to +1.13 V in $CH_3CN$) corresponding to generation of $DMA^+$. After reversing the sweep, no reduction wave for $DMA^+$ is observed; rather a new peak, 2, appears whose "spike" shape is characteristic of a species strongly interacting with the electrode surface. At sweep rates between 0.2 and 1.0 V/sec,

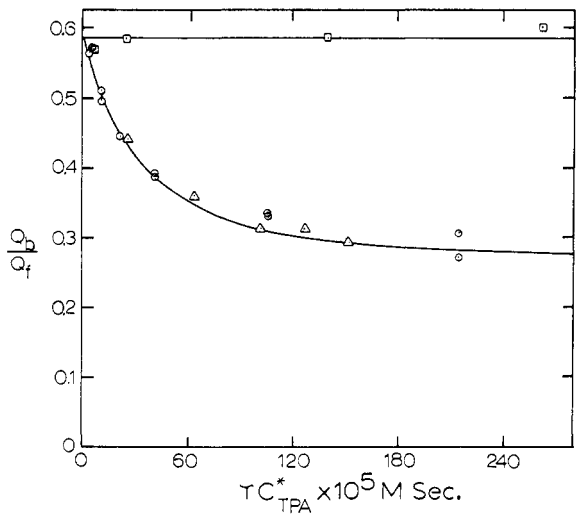


**Figure 11. Double-potential step chronocoulometry of triphenylamine in butyronitrile containing 0.1*M* TBAP at a platinum electrode**

**Potential step amplitude: +0.6 V to +1.4 V *vs.* SCE**
**⊙ 4.35m*M* triphenylamine at 298 °K**
**△ 2.62m*M* triphenylamine at 298 °K**
**□ 2.62m*M* triphenylamine at 183 °K**

(51) T. C. Werner, J. Chang, and D. M. Hercules, *J. Amer. Chem. Soc.*, **92**, 763 (1970).
(52) T. A. Gough and M. E. Peover, "Polarography—1964," Macmillan, New York, N.Y., 1966, p 1017.
(53) V. D. Parker, *Chem. Commun.*, **1969**, 848.
(54) V. D. Parker and L. Eberson, *Tetrahedron Lett.*, **33**, 2830 (1969).

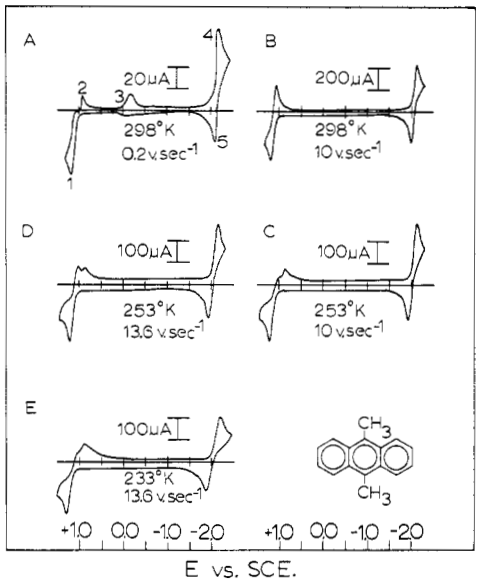


**Figure 12. Steady-state cyclic voltammograms of 9,10-dimethylanthracene on a platinum electrode at room temperature and low-temperatures. 2.72m*M* 9,10-dimethylanthracene and 0.1*M* TBAP in butyronitrile**

the $DMA^+$ to DMA reduction wave can be observed and peak 2 is diminished. At 10 V/sec (Figure 12*B*) a perfectly reversible one-electron wave is observed for the oxidation of DMA. Thus peak 2 is identified as a product wave resulting from the cation radical decay process. The voltammetric wave near 0.0 V is attributed to free protons liberated by the decay chemistry of $DMA^+$. The redox process consisting of waves 4 and 5 is the $DMA^+$/DMA couple. The peak current ratio for the anion radical couple, $i_p^a/i_p^c$, is less than unity due to the protonation reactions, Hoijtink mechanism (ECEC), of $DMA^-$ by the $H^+$ formed by $DMA^+$ decay. If the potential sweep had been initiated in the negative direction so that $DMA^+$ was generated first, $i_p^a/i_p^c = 1.00$ would have been observed as expected. At moderately high sweep rates as in Figure 12*B*, the proton wave 3 is absent, again indicating insufficient time for the cation radical decay reaction to occur. Additionally, the cation radical lifetime is highly DMA concentration dependent. At low DMA concentration (*ca.* 0.5m*M*), $DMA^+$ is somewhat stable ($i_p^c/i_p^a = 0.7$ at 0.20 V/sec.); whereas, at high concentration (5 m*M*) no reverse wave for cation radical recovery is observed even at 25 V/sec. Thus we conclude that $DMA^+$ is *not* stable in butyronitrile; a result that was not in accord with our expectations or previous experience with other hydrocarbon oxidations and is in complete contradiction with the oxidative behavior of DMA in acetonitrile.

These voltammetric results for DMA oxidation can be interpreted in terms of the simple scheme:

$$DMA \rightleftharpoons DMA^+ + e^- \quad (9)$$

$$2\ DMA^+ \xrightarrow{k} \text{product(s)} + n\ H^+ \quad (10)$$

or

$$DMA + DMA^+ \xrightarrow{k} \text{product(s)} + n\ H^+ \quad (11)$$

where the second-order follow-up reaction accounts for the DMA concentration dependence of the cation radical lifetime, peak 3 is accounted for by the release of protons in the decay reaction, and peak 2 is the reduction of a product formed in Equations 10 or 11. The peak current function $i_p^a\ V^{-1/2}/C$ for DMA oxidation decreases slightly with increasing sweep rate indicating either: the product(s) are nonelectroactive (*i.e.*, 2nd order EC mechanism); or only a small fraction of the total product mixture is susceptible to further electron transfer. With the data presently at hand we are unable to distinguish the cation dimerization scheme, Reaction 10, from the cation radical/parent interactions mechanism, Reaction 11.

The low-temperature behavior of the DMA oxidation produces an even more remarkable result. Cooling the system to 253 °K (Figure 12*C*) while cycling between +1.3 and −2.3 V *vs.* SCE at 10 V/sec, so that both DMA reduction and DMA oxidation are reversible one-electron transfers, resulted in a *DECREASE* in the DMA radical cation lifetime accompanied by the appearance of product peak 2. Increasing the sweep rate slightly to 13.6 V/sec at the same temperature (Figure 12*D*) increases the recovery of cation radical and cooling again to 233 °K at constant sweep rate (Figure 12*E*) results in another decrease in the cation radical life lifetime. At very low temperatures (183 °K), no cation radical could be recovered on the reverse sweep at the fastest sweep rate available at that temperature (*ca.* 50 V/sec.). Avoiding explanations involving an anti-Arrhenius temperature dependence for the cation radical decay reaction, an equilibrium decay reaction is proposed:

$$2\ DMA^+ \underset{k_b}{\overset{k_f}{\rightleftharpoons}} \text{product(s)} + n\ H^+ \quad (12)$$

or

$$DMA + DMA^+ \underset{k_b}{\overset{k_f}{\rightleftharpoons}} \text{product(s)} + n\ H^+ \quad (13)$$

where $K_{eq} = k_f/k_b$.

The observed decrease in cation radical lifetime can, therefore, be explained as a low-temperature shift in the follow-up reaction equilibrium constant such that the product state is preferred at low-temperatures. In thermodynamic terms, this means that the DMA cation radical decay reaction is exothermic which is equivalent to the kinetic statement that the activation energy of the forward reaction is less than the activation energy of the back reaction. Furthermore, the dramatic dependence of cation radical lifetime on solvent can now be explained by a similar equilibrium constant shift in the decay reaction induced by the solvent dielectric constant change in going from acetonitrile ($\epsilon = 36.7$) to butyronitrile ($\epsilon = 20.3$). This explanation is plausible provided the degree of charge separation in the products is less than that for the free cation radical.

It is tempting to speculate that dimeric species such as IV (with $H_2O$ replacing acetate as the nucleophile) or V are the products of the $DMA^+$ decay reaction. An even more intriguing possibility is that the equilibrium decay reaction goes through a dimer cation radical intermediate resulting from a monomer cation radical/parent interaction, viz.:

$$DMA + DMA^+ \underset{k_{-1}}{\overset{k_1}{\rightleftharpoons}} (DMA)_2^+ \xrightarrow{k_2} \text{product(s)} + n\ H^+ \quad (14)$$

Dimer cation radicals of anthracene naphthalene, and 2,3,6,7-tetramethylnaphthalene have been obtained by low-temperature oxidation of the substrates with $SbCl_5$ in $CH_2Cl_2$ and observed by ESR (*55*, *56*). Dimer cation radicals have also been assigned to optical absorption bands in the spectra of

(55) O. W. Howarth and G. K. Fraenkl, *J. Chem. Phys.*, **52**, 6258 (1970).
(56) I. C. Lewis and L. S. Singer, *ibid.*, **43**, 2712 (1965).

certain aromatic hydrocarbons in $\gamma$-irradiated low-temperature glasses (*57*, *58*). Additionally it has recently been shown that the cation radical of magnesium octaethylporphyrin (*59*) undergoes a low-temperature dimerization in methanol over the temperature range 0 to −60 °C. At present, we have no evidence with which to support or refute any of these product speculations. Suffice it to say that these studies will continue and that the 9,10-DMA oxidation system has provided the first clear example of a situation in which low-temperature electrochemical studies have provided a new and highly provocative piece of electrode reaction mechanistic information that was not readily available from room temperature electrochemical studies alone.


(57) B. Badger, B. Brocklehurst, and R. D. Russell, *Chem. Phys. Lett.*, **1**, 122 (1967).
(58) B. Badger and B. Brocklehurst, *Trans. Faraday Soc.*, **65**, 2576, 2582, 2588 (1969).
(59) J. Fajer, D. C. Borg, A. Forman, D. Dolphin, and R. H. Felton, *J. Amer. Chem. Soc.*, **92**, 3451 (1970).



ACKNOWLEDGMENT

Dr. Peter Kissinger provided assistance with spectral monitoring of the diphenylanthracene regeneration reaction and many helpful discussions.

RECEIVED for review March 29, 1971. Accepted August 2, 1971. One of the authors (R.P.V.D.) wishes to acknowledge support of a National Aeronautics and Space Administration Fellowship (1967–1970). Various aspects of this work was supported by the Advanced Research Projects Agency under Contract SD-100 with the U.N.C. Materials Research Center and by the Air Force Office of Scientific Research (AFSC), USAF, under Grant AF-AFOSR-69-1625.


# Stability Constants of Tin–Pyrocatechol Violet Complexes from Computer Analysis of Absorption Spectra


**William D. Wakley[1] and Louis P. Varga[2]**

*Department of Chemistry and Reservoir Research Center, Oklahoma State University, Stillwater, Okla. 74074*



**By systematic computer analysis of spectral data, the number of absorbing species, the stoichiometry, and the equilibrium constants of the tin(IV)–pyrocatechol violet system were determined in 1*M* aqueous chloride solution. The acid dissociation constants of pyrocatechol violet determined in this medium were: $pK_1 = 0.26 \pm 0.01$, $pK_2 = 7.51 \pm 0.01$, $pK_3 = 8.33 \pm 0.02$, with $pK_4$ not determined. In the presence of 1 to $4 \times 10^{-5}$*M* tin(IV) chloride at pH = 3.0, absorbance data over the wavelength range 660 to 265 nm were interpreted in terms of the formation, from $H_3L^-$, of 1:1, 1:2, and 2:1 $Sn^{4+}$:$H_2L^{2-}$ complexes with log $^*\beta_{11} = 7.80 \pm 0.13$, log $^*\beta_{12} = 14.90 \pm 0.30$, and log $^*\beta_{21} = 12.92 \pm 0.34$. Molar absorptivities of all species were determined as a function of wavelength. Both $SnH_2L^{2+}$ and $Sn(H_2L)_2$ showed maximum absorbance at 555 nm, with molar absorptivities, 33,730 and 79,620 $cm^{-1}$ $mole^{-1}$ liter, respectively. Some possible structures of the ligand and of the metal–ligand complexes are discussed. A modification of Sillen's general least squares "pit-mapping" program, in conjunction with absorbance matrix rank, corresponding solution, and mole-ratio methods, was used in the analysis. The calculation methodology embodied in these programs proved to be a powerful tool for the interpretation of solution spectra in equilibrium systems.**


STUDIES OF THE ABSORPTION of visible and ultraviolet radiation have long been used to obtain information on complex ion equilibria in solution. However, many spectrophotometric methods used in quantitative analysis have been developed without much knowledge of the equilibria involved or of the structure of the absorbing species. Since the absorbance of a solution is governed by a characteristic intensive factor, the absorptivity, as well as by the concentration of each absorbing species, interpretation of measurements of this type is complicated if several chromophores coexist. Mathematical models used to describe the systems are usually nonlinear in the unknown coefficients so that iterative least-squares and graphical methods often are used in these studies to interpret the data. If the systems under study are "ill-conditioned" such that phase space in the area of the least-squares minimum is flat or if several local minima are present, then the accuracy and precision of the experimental data are not sufficient to produce unambiguous results except in the simplest cases. Under these conditions, careful stepwise interpretive techniques in addition to more powerful mathematical tools are needed. As shown below, progress in this area is encouraging.

Reagents for tin listed by Sandell (*1*) have been described as generally unsatisfactory in sensitivity and specificity. Dithiol was considered the most useful followed by phenylfluorone (*2–4*). The spectrophotometric method for tin suggested by Ross and White (*5*) using pyrocatechol violet (PCV, pyrocatechol sulfonphthalein, or 3,3′,4′-trihydroxyfuchsone-2″-sulfonic acid) was described as quite sensitive and less subject to errors that previous procedures. PCV appeared to form at least two complexes with tin(IV) at a recommended pH of 3, but no information was given regarding the nature or stabilities of these complexes. Since several metal ions have been reported to form stable chromogenic complexes with PCV at high acidities (*6*), the nature and stabilities of the tin(IV) complexes were of particular interest in these laboratories in studies on general methods

[1] Present address, Department of Physical Science, Tulsa Junior College, Tulsa, Okla.
[2] To whom reprint requests should be made.


(1) E. B. Sandell, "Colorimetric Determination of Traces of Metals," Interscience, New York, N. Y., 1959.
(2) R. L. Bennett and H. A. Smith, ANAL. CHEM., **31**, 1441 (1959).
(3) C. L. Luke, *ibid.*, **28**, 1276 (1956).
(4) *Ibid.*, **31**, 1803 (1959).
(5) W. J. Ross and J. C. White, *ibid.*, **33**, 421 (1961).
(6) V. Suk and M. Malat, *Chemist-Analyst*, **45**, 30 (1956).